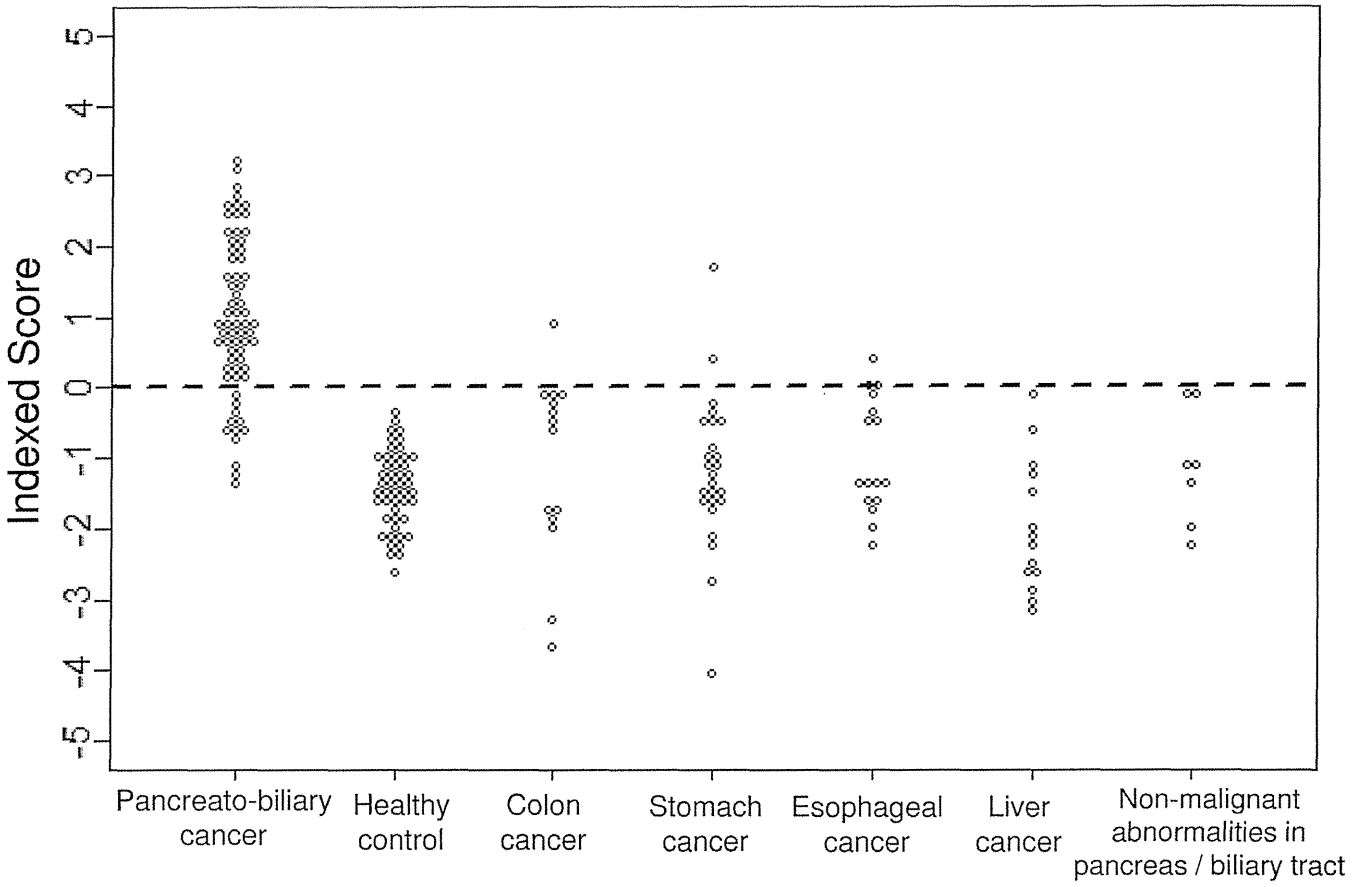

Fig 5. Indexed scores that gave the best discriminant performance in the test cohort with the use of four miRNAs: miR-6075, miR-6799-5p, miR-125a-3p, and miR-6836-3p.

doi:10.1371/journal.pone.0118220.g005

the diagnostic power of this index was not affected by tumor location of either pancreatic or biliary-tract cancer.

On the other hand, 5 of 29 pancreatic cancers and 7 of 37 biliary-tract cancers in the test cohort gave false-negative scores by the miRNA index. These false-negative cases did not show any partiality in their clinical characteristics; between the false-negative and the true-positive cases, there was no significant difference in the patients' age ($p = 0.111$), serum CA19-9 ($p = 0.581$) or CEA ($p = 0.063$) concentrations nor was there a difference in the histological location of the tumor or the sites of distant metastasis. Similarly, 4 of 124 control samples gave false-positive scores by the miRNA index. The false-positive samples varied in their clinical status (One colon cancer, 1 esophageal cancer, 2 stomach cancers) and did not show any particular clinical characteristics that might indicate any bias. There was one non-malignant abnormality case that was initially diagnosed as chronic pancreatitis, but after 3-year follow-up, pancreatic cancer was found. This case was designated in the training cohort, and was negative by both CEA (1.2 ng/mL) and CA19-9 (10 U/mL) test, but positive by our diagnostic index.

These results suggest that the diagnostic index is able to detect pancreato-biliary cancers at various stages and histological locations, and discriminates not only against healthy individuals

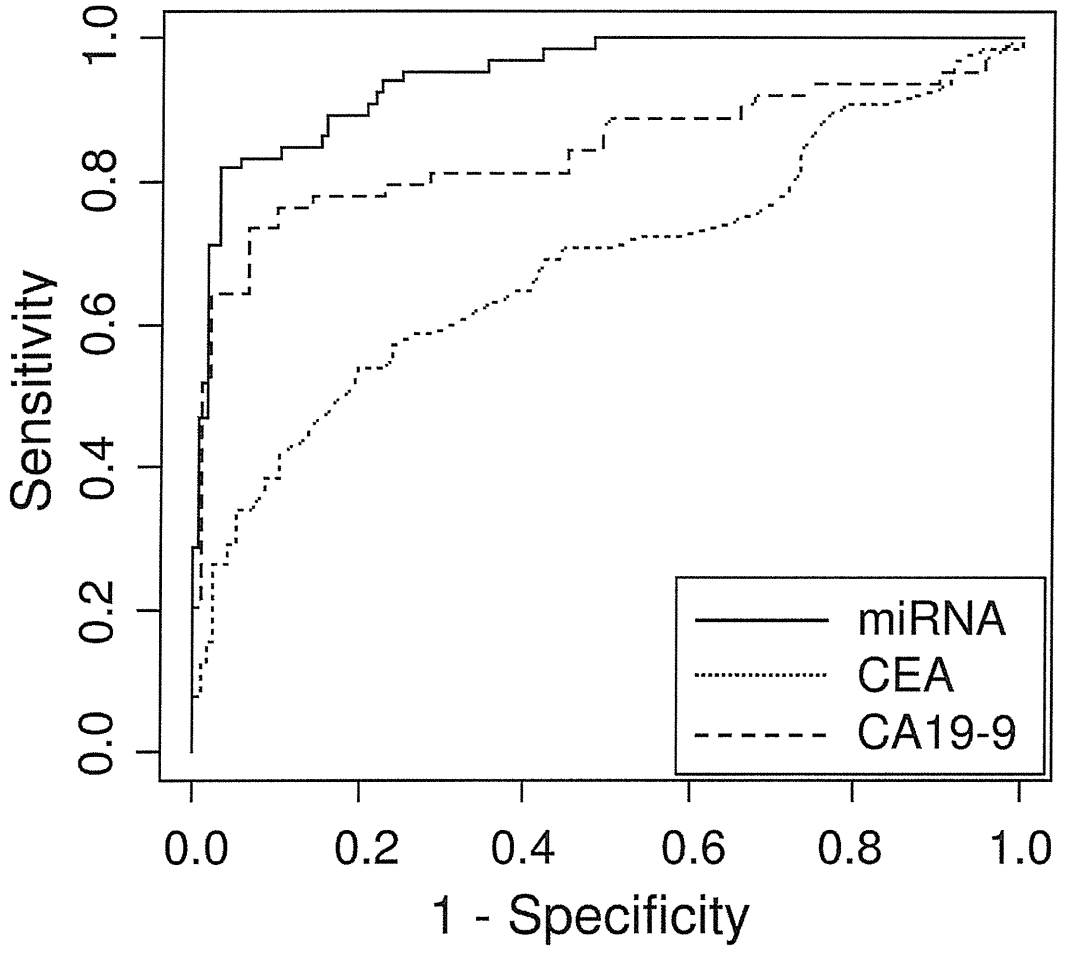

Fig 6. ROC analysis of a combination of four miRNAs (miR-6075, miR-6799-5p, miR-125a-3p, and miR-6836-3p) in a solid line, CEA in a dotted line, and CA19-9 in a slashed line. The AUC values were 0.949, 0.682 and 0.845 for a combination of the four miRNAs, CEA, and CA19-9, respectively. The analysis was performed in the test cohort.

doi:10.1371/journal.pone.0118220.g006

but also against individuals with non-malignant abnormalities in pancreato-biliary organs as well as those with other types of cancers.

Validation of the miRNA expression in normal and cancerous tissues of the pancreas

The expression of the miRNAs selected for the diagnostic indices was validated in the FFPE tissue samples obtained from 10 patients with pancreatic cancer. Paired samples of cancerous tissue and the surrounding normal tissue were separately obtained from the same patients by macroscopic-dissection. The expression of those ten miRNAs that were used in the discriminant index was quite strong in the pancreatic cancer tissue (all within the top 10% of miRNAs in terms of the median expression signals); however, they did not show statistical significance in differentiating the cancerous tissue from the normal surrounding tissue (Table 5), indicating that miRNA markers obtained from serum samples may not comparable with those obtained from corresponding tissue samples.

Table 4. The number of positive and negative samples by CEA, CA19-9, and the diagnostic index* tests in each clinical group.

	Clinical group	Stage or operability	CEA (median)		CA19-9		Diagnostic Index*	
			Positive	Negative	Positive	Negative	Positive	Negative
Training cohort (381)	Healthy control (102)	-	4	98	3	99	0	102
	Pancreatic cancer (71)	pStage I	0	0	0	0	0	0
		pStage II	2	11	9	4	12	1
		cStage III	9	12	16	5	19	2
		cStage IV	25	12	30	7	34	3
	Biliary-tract cancer (61)	Operable	6	20	14	12	21	5
		Inoperable**	14	20	28	5	27	8
	Non-malignant abnormalities in pancreas or biliary tract (14)	-	2	12	3	11	6	8
	Colon cancer (36)	-	12	24	6	30	11	25
	Stomach cancer (25)	-	2	23	4	21	2	23
	Esophageal cancer (34)**	-	5	28	-	-	9	25
	Liver cancer (38)**	-	4	17	3	5	5	33
Test cohort (176)	Healthy control (48)	-	2	46	0	48	0	48
	Pancreatic cancer (29)	pStageI	1	0	1	0	1	0
		pStageII	1	4	3	2	3	2
		cStageIII	3	3	5	1	5	1
		cStageIV	11	6	13	4	15	2
	Biliary-tract cancer (37)	Operable**	3	18	10	10	17	5
		Inoperable	7	8	10	5	13	2
	Non-malignant abnormalities in pancreas or biliary tract (7)	-	2	5	1	6	0	7
	Colon cancer (14)	-	4	10	3	11	1	13
	Stomach cancer (25)	-	1	24	3	22	2	23
	Esophageal cancer (16)**	-	2	14	-	-	1	15
	Liver cancer (14)**	-	3	10	0	4	0	14

*The diagnostic index used the following four miRNAs: miR-6075, miR-6799-5p, miR-125a-3p, and miR-6836-3p.

**CA19-9 and/or CEA scores were not available in some cases of biliary-tract cancer, esophageal cancer, and liver cancer.

doi:10.1371/journal.pone.0118220.t004

Discussion

Despite the desperate need for the early detection of pancreatic cancer, there is no simple, least-invasive screening method. Pancreatic cancer has such a low prevalence in general population that it may be difficult even for accurate diagnostic tests to achieve sufficient positive-predictive values in population-wide screening [13]. Since imaging tests still have their limitations in diagnosis of pancreatic cancers, particularly of those at early stages [2, 14], development of novel blood marker tests for pancreatic cancer is urgently needed.

The current blood biomarkers CEA and CA19-9 have been prevalently used for post-operation monitoring, but their poor specificity for non-malignant diseases and other cancers as well as their poor sensitivities to early cancers prevent them from being widely used in screening systems. In this study, CEA and CA19-9 failed to detect not only the early stage of pancreatic and biliary-tract cancers but also progressed cancers. A simple blood screening-test alternative to those protein markers is necessary for pancreato-biliary cancers.

Several prior studies have shown the value of serum miRNAs in the detection of several kinds of cancers [5–9, 15, 16]. A number of new cancer-related miRNAs have been recently

Table 5. Expression of the ten miRNAs used in the discriminant indices in paired malignant and normal tissues obtained from the same patients with pancreatic cancer (n = 10).

miRNA	Expression Signal (Median)		p-value
	Normal (n = 10)	Tumor (n = 10)	
miR-6075	11.3	11.2	5.9.E-01
miR-4294	8.8	9.0	6.2.E-01
miR-6880-5p	8.4	8.5	8.6.E-01
miR-6799-5p	10.7	10.0	8.3.E-02
miR-125a-3p	10.1	9.8	1.5.E-01
miR-4530	12.9	12.7	1.0.E-01
miR-6836-3p	7.6	7.3	1.9.E-01
miR-4634	8.7	8.5	1.2.E+00
miR-7114-5p	10.0	9.9	2.2.E+00
miR-4476	8.0	8.0	8.3.E-01

doi:10.1371/journal.pone.0118220.t005

identified, and most of them have never been examined in pancreatic cancer. In this study, using highly sensitive microarrays that permitted the simultaneous analysis of more than 2,500 miRNAs that were recently updated in the miRBase (release 20), we examined the expression profiles of comprehensive serum miRNAs in patients with pancreato-biliary cancers. In addition to 100 patients with pancreatic cancer and 98 patients with biliary-tract cancer, we examined 150 healthy control individuals, 21 patients with non-malignant abnormalities in either the pancreas or the biliary tract, and 202 patients with other types of cancers (esophagus, stomach, liver, and colon) to determine the discriminant performance in various clinical settings, allowing us to study the markers in the largest and most comprehensive clinical cohort that has yet been attempted. Especially, the study setting with the control cohort that is consisted of diverse populations is critical when envisaging the implementation of biomakers in real clinical setting. At first, we tried to discover serum miRNA markers for pancreatic cancer, and we obtained 81 miRNAs in a comparative analysis with healthy controls. However, 55 of those miRNAs (67.9%) were also markers that discriminated between biliary-tract cancers and healthy control samples. That finding suggested that the exclusive identification of pancreatic cancers and biliary-tract cancers, respectively, by serum miRNA was so difficult that we decided to find markers that detect pancreatic and biliary-tract cancers simultaneously. Those results had led to our concern that any cancer type would show similar miRNA expression profiles in the serum, and that we would be unable to discriminate other cancer types from pancreato-biliary malignancies. We therefore additionally prepared samples of other types of digestive-tract cancers. Furthermore, we prepared samples from patients with non-malignant abnormalities, because CA19-9, the most frequently used biomarker for pancreatic cancer, is known to be expressed in non-malignant abnormalities such as inflammation, leading to poor specificity toward that clinical group.

In this study, the best single marker achieved an accuracy of 84.7% in detecting pancreato-biliary cancers. By combining multiple significant miRNAs, we had thought to attain higher diagnostic performance as previously demonstrated [17, 18]. Utilizing the 10 most significant miRNAs deduced from the above comparative analyses, diagnostic indices were developed, and their discriminant performance was validated in the test cohort. By combining 8 miRNAs (miR-6075, miR-4294, miR-6880-5p, miR-6799-5p, miR-125a-3p, miR-4530, miR-6836-3p, and miR-4476) out of the 10 miRNA selected, we finally achieved the best discriminant performance with a sensitivity of 80.3%, a specificity of 97.6%, and an accuracy of 91.6% in detecting

pancreato-biliary cancers among healthy control, non-malignant abnormalities or other types of cancers. When more miRNAs (in this case, nine or more) were integrated into the diagnostic indices, the discriminant performance started to decline, possibly due to the pick-up of noise features. Such a phenomenon is known as the "curse of dimensionality" in algorithm development [19].

We further validated the detailed result of the discriminant function composed of four miRNAs (the combination with the least number of miRNAs). The detailed validation of the discriminant performance revealed the clinical value of the diagnostic index; the index identified the early phase of pancreato-biliary cancers that were surgically resectable. Because the current best treatment for pancreato-biliary cancers is the resection of tumors while the tumors are still localized in the organs, a diagnostic index capable of detecting small resectable tumors is promising. Furthermore, this index was able to detect any histological type of tumors, some of which (e.g., tumors located in the pancreatic tail or the intrahepatic bile duct) could be difficult to detect by image screening if not well attended. This index which utilizes blood miRNA markers could be used beforehand to provide a rationale to perform more costly and/or invasive screening tests such as a CT scan or endoscopic ultrasound.

Although we found that a combination of serum miRNAs could become a specific marker for pancreato-biliary cancers, the biological roles of those serum miRNAs are under discussion. Nine out of the ten miRNAs used for the diagnostic indices had an ID name higher than 1,000, indicating that they were discovered relatively recently. We were therefore not able to find many references about those miRNAs except for miR-125a-3p. Serum miR-125a-3p has been reported to show different expression profiles between patients with pancreatic cancers and healthy individuals [5, 7]. In the current study, we also found that miR-125a-3p is a strong candidate for the detection of pancreato-biliary cancers in the independent analysis. However, the integrated analysis showed that miR-125a-3p was differentially expressed in sera from patients with other digestive-tract cancers as well, indicating that that miRNA is not a cancer type-specific marker but is instead a broad marker similar to CEA or CA19-9.

One of the mRNAs targeted by miR-125a-3p is MYST/Esa1-associated factor 6 (MEAF6), which encodes a nucleic protein that is associated with transcriptional activators. It is reported that MEAF6 binds with NuF4 complex, which acetylates histone H4 [20]; and this NuF4 complex is known to interact with the oncogenic transcriptional regulator c-Myc [21]. It could be hypothesized that the decreased miR-125a-3p expression leads to a reduction of the repressing effect on the above oncogenes, promoting carcinogenesis.

It is hypothesized that cancer cells secrete exosomes that encompass various molecular informants including proteins, DNA, and miRNAs into the blood stream and send them to distant organs in order to cultivate a new environment for future metastasis [15, 16]. According to this hypothesis, sera from patients with cancer should contain more miRNAs than those from healthy individuals; however, we did not observe such a phenomenon based on the overall expression-signal intensity obtained from the same 300-μL serum samples. In fact, the expression levels of seven out of ten miRNA markers (miR-6075, miR-4294, miR-6880-5p, miR-6799-5p, miR-125a-3p, miR-4530, miR-6836-3p, miR-4634, miR-7114-5p, miR-4476) used for the diagnostic indices were decreased in the serum samples from the patients with cancer compared with those from the healthy control individuals. Therefore, other biological cascades should also be considered for the secretion of circulating miRNAs.

Another enigma is the discordance of miRNA expression profiles in the serum and in the tissues. The 10 miRNAs that were significantly expressed in the sera of the patients with pancreato-biliary cancers did not show similar significant increases in the FFPE cancerous tissues compared with the surrounding normal tissues. This observation is again not in accordance with the tumor-secreted exosome theory. We think that the underlying mechanism of

circulating miRNAs is more complex than previously speculated. Furthermore, we have preliminary data indicating that expression profiles of those miRNAs that were especially derived from clinical samples such as blood or FFPE tend to fluctuate depending on the assay method (microarray, PCR, sequencer) used (data not shown). In short, a number of studies remain to be performed to elucidate the biological significance of the miRNAs that we found to be involved in pancreatic and biliary-tract carcinogenesis. Until such a mechanism is clarified, the serum miRNA markers for pancreato-biliary cancers should not be confused with the tissue miRNA markers.

In conclusion, our results provide strong data showing that serum miRNAs, particularly diagnostic index conducted by the combination of several predictive miRNAs, can detect patients with pancreatic and biliary-tract cancers against a background of those who are healthy, have other non-malignant diseases or have other types of cancer. We believe that detecting pancreato-biliary cancers using peripheral blood, which is relatively easy to obtain from most subjects, is clinically useful, particularly as a first screening test. Such a test will provide additional information to those who could be at risk and, if necessary, encourage them to take more costly, sometimes invasive, imaging tests. We hope that such a test will lead to the early detection of these cancers and to improvement in the currently devastating survival rate.

Supporting Information

S1 Table. Validated miRNA markers that differentiate between patients with pancreatic cancer and healthy control individuals (A) or patients with biliary-tract cancer and healthy control individuals (B).
(DOCX)

S2 Table. Best discriminate functions for each possible number of miRNAs used in the test cohort.
(DOCX)

Author Contributions

Conceived and designed the experiments: MK HS JK ST SK HN AO. Performed the experiments: JK HS. Analyzed the data: MK HS JK ST SK HN AO. Contributed reagents/materials/analysis tools: MK HS JK ST SK HN AO. Wrote the paper: MK HS JK ST SK HN AO.

References

1. American Cancer Association. Pancreatic Cancer Last Medical Review 11 June 2014. Web 1 July 2014. <http://www.cancer.org/acs/groups/cid/documents/webcontent/003131-pdf.pdf>
2. Brand B, Pfaff T, Binmoeller KF, Sriram PV, Fritscher-Ravens A, et al. (2000) Endoscopic ultrasound for differential diagnosis of focal pancreatic lesions, confirmed by surgery. Scand J Gastroenterol. 35(11):1221–8. PMID: 11145297
3. Ballehaninna UK, Chamberlain RS (2012) The clinical utility of serum CA 19–9 in the diagnosis, prognosis and management of pancreatic adenocarcinoma: An evidence based appraisal. J Gastrointest Oncol. 3(2):105–19. doi: 10.3978/j.issn.2078-6891.2011.021 PMID: 22811878
4. Morris-Stiff G, Taylor MA (2012) Ca19-9 and pancreatic cancer: Is it really that good? Gastrointest Oncol. 3(2):88–9.
5. Ali S, Almhanna K, Chen W, Philip PA, Sarkar FH (2010) Differentially expressed miRNAs in the plasma may provide a molecular signature for aggressive pancreatic cancer. Am J Transl Res. 2010 Sep 28; 3(1):28–47. PMID: 21139804
6. Ganepola GA, Rutledge JR, Suman P, Yiengpruksawan A, Chang DH (2014) Novel blood-based microRNA biomarker panel for early diagnosis of pancreatic cancer. World J Gastrointest Oncol. 6(1):22–33. doi: 10.4251/wjgo.v6.i1.22 PMID: 24578785

7. Li A, Yu J, Kim H, Wolfgang CL, Canto MI, et al. (2013) MicroRNA array analysis finds elevated serum miR-1290 accurately distinguishes patients with low-stage pancreatic cancer from healthy and disease controls. Clin Cancer Res. 19(13):3600–10. doi: 10.1158/1078-0432.CCR-12-3092 PMID: 23697990

8. Liu J, Gao J, Du Y, Li Z, Ren Y, et al. (2012) Combination of plasma microRNAs with serum CA19-9 for early detection of pancreatic cancer. Int J Cancer. 131(3):683–91. doi: 10.1002/ijc.26422 PMID: 21913185

9. Liu R, Chen X, Du Y, Yao W, Shen L, et al. (2012) Serum microRNA expression profile as a biomarker in the diagnosis and prognosis of pancreatic cancer. Clin Chem. 58(3):610–8. doi: 10.1373/clinchem.2011.172767 PMID: 22194634

10. Smyth GK (2005) Limma: linear models for microarray data. In: Bioinformatics and Computational Biology Solutions using R and Bioconductor, Gentleman R., Carey V., Dudoit S., Irizarry R., Huber W. (eds.), Springer, New York, pages 397–420.

11. Venables WN, Ripley BD (2002) Modern Applied Statistics with S. Fourth Edition. Springer, New York. PMID: 25057650

12. Eklund A (2013) beeswarm: The bee swarm plot, an alternative to stripchart. <http://CRAN.R-project.org/package=beeswarm>

13. Becker AE, Hernandez YG, Frucht H, Lucas AL (2014) Pancreatic ductal adenocarcinoma: Risk factors, screening, and early detection. World J Gastroenterol. 20(32):11182–11198. doi: 10.3748/wjg.v20.i32.11182 PMID: 25170203

14. Bartsch DK, Gress TM, Langer P (2012) Familial pancreatic cancer—current knowledge. Nat Rev Gastroenterol Hepatol. 9(8):445–53. doi: 10.1038/nrgastro.2012.111 PMID: 22664588

15. Challagundla KB, Fanini F, Vannini I, Wise P, Murtadha M, et al. (2014) microRNAs in the tumor microenvironment: solving the riddle for a better diagnostics. Expert Rev Mol Diagn. 14(5):565–74. doi: 10.1586/14737159.2014.922879 PMID: 24844135

16. Kosaka N, Yoshioka Y, Hagiwara K, Tominaga N, Katsuda T, et al. (2013) Trash or Treasure: extracellular microRNAs and cell-to-cell communication. Front Genet. 4:173. doi: 10.3389/fgene.2013.00173 PMID: 24046777

17. Taguchi YH, Murakami Y (2013) Principal component analysis based feature extraction approach to identify circulating microRNA biomarkers. PLoSOne. 8(6):e66714. doi: 10.1371/journal.pone.0066714 PMID: 23874370

18. Sato F, Hatano E, Kitamura K, Myomoto A, Fujiwara T, et al. (2011) MicroRNA profile predicts recurrence after resection in patients with hepatocellular carcinoma within the Milan criteria. PLoSOne. 6(1):e16435. doi: 10.1371/journal.pone.0016435 PMID: 21298008

19. Lee G, Rodriguez C, Madabhushi A (2008) Investigating the efficacy of nonlinear dimensionality reduction schemes in classifying gene and protein expression studies. IEEE/ACM Trans Comput Biol Bioinform. 5(3):368–84. doi: 10.1109/TCBB.2008.36 PMID: 18670041

20. Doyon Y1, Selleck W, Lane WS, Tan S, Côté J (2004) Structural and functional conservation of the NuA4 histone acetyltransferase complex from yeast to humans. Mol Cell Biol. 24(5):1884–96. PMID: 14966270

21. Kim J1, Woo AJ, Chu J, Snow JW, Fujiwara Y, et al. (2010) A Myc network accounts for similarities between embryonic stem and cancer cell transcription programs. Cell 143(2):313–24. doi: 10.1016/j.cell.2010.09.010 PMID: 20946988

Cancer Science
Japanese Cancer Association JCA
Open Access

Spread of tumor microenvironment contributes to colonic obstruction through subperitoneal fibroblast activation in colon cancer

Mitsuru Yokota,[1,2] Motohiro Kojima,[3] Youichi Higuchi,[4] Yuji Nishizawa,[1] Akihiro Kobayashi,[1] Masaaki Ito,[1] Norio Saito[1] and Atsushi Ochiai[3]

[1]Division of Colorectal Surgery, Research Center for Innovative Oncology, National Cancer Center Hospital East, Kashiwa; [2]Department of Surgery, School of Medicine, Keio University, Tokyo; [3]Division of Pathology, Research Center for Innovative Oncology, National Cancer Center Hospital East, Kashiwa; [4]Laboratory of Cancer Biology, Department of Integrated Biosciences, Graduate School of Frontier Sciences, The University of Tokyo, Tokyo, Japan

Key words
Colon cancer, elastic laminal invasion, fibroblast, obstruction, tumor microenvironment

Correspondence
Atsushi Ochiai, Division of Pathology, Research Center for Innovative Oncology, National Cancer Center Hospital East, 6-5-1 Kashiwanoha, Kashiwa 277-8577, Japan.
Tel: +81-4-7133-1111; Fax: +81-4-7131-9960;
E-mail: aochiai@east.ncc.go.jp

Funding Information
Japan Society for the Promotion of Science.

Received November 4, 2014; Revised January 3, 2015; Accepted January 14, 2015

Cancer Sci (2015)

doi: 10.1111/cas.12615

We evaluated the influence of the cancer microenvironment formed by peritoneal invasion (CMPI) on clinical findings in colon cancer patients. In addition to the association with poor prognosis, we discovered a relationship with bowel obstruction. Detailed analysis revealed that clinical findings related to bowel obstruction occurred more frequently in patients with an elevated type tumor, which had peritoneal elastic laminal elevation to the tumor surface, compared to those with non-elevated type tumors among those with elastic laminal invasion (ELI). Lateral tumor spread and increase of tumor annularity rate in ELI-positive elevated type cases suggested the morphological progression from ELI-positive non-elevated type to elevated type. In addition, α-smooth muscle actin expression was the highest in ELI-positive elevated type, and prominent expressions were found not only in the deep tumor area but also in the shallow tumor area. Furthermore, contraction assays revealed the robust contractile ability of subperitoneal fibroblasts stimulated by cancer cell-conditioned medium. Our findings suggest that CMPI spread into the luminal side of the colonic wall along with tumor progression, which caused bowel obstruction through the activation of subperitoneal fibroblasts. However, although the clinical outcome was not different between the two types, the clinical findings were affected by the spread of CMPI. We are the first to explore how the alteration of the tumor-promoting microenvironment, along with tumor progression, contributes to the development of clinical findings.

Colorectal cancer (CRC) is one of the most frequent malignancies in the world.[1–3] The majority of patients with early stage CRC have no symptoms and their cancers are often detected during colorectal screening. However, in spite of the development of the screening system, there are still many patients whose cancers are diagnosed in an advanced stage with clinical findings such as melena, abdominal pain, or obstruction.[4,5] Clinical findings related to CRC are caused by tumor growth into the intestinal lumen and tumor invasion to the adjacent organs, therefore the development of clinical findings typically occurs in relatively advanced stage CRC. Nevertheless, not all patients with advanced stage CRC experience clinical findings. For instance, patients with an apple-core lesion on barium enema examination do not always show obstructive symptoms and there may be no difficulty in passage of the colonoscope despite a typical annular severe stricture formation. Thus, the relationship between clinical findings and tumor progression remains unclear.

Recently, peritoneal elastic laminal invasion (ELI) was reported to be a strong prognostic factor in colon cancer (CC).[6–8] Furthermore, we reported that the cancer microenvironment formed by the peritoneal invasion (CMPI) promoted tumor progression and metastasis through the interaction between subperitoneal fibroblasts (SPFs) and cancer cells.[9] Peritoneal tissue is one of the final layers of the colonic wall, so ELI occurred in advanced stage CC. In addition, marked morphological and pathological alterations were observed in tumor tissues after ELI. Therefore, ELI, and CMPI formed after ELI, may cause CC-related clinical findings. In this study, we aimed to evaluate how the formation of the tumor microenvironment, such as CMPI, could change the characteristics of the tumor tissue, and whether it could affect clinical findings. Using detailed morphometrical and biological investigation, we evaluated the interaction between SPFs and cancer cells within CMPI in colonic obstruction.

Materials and Methods

Patient selection and follow-up. A total of 205 patients with pT3 and pT4a CC who underwent curative surgery at the National Cancer Center Hospital East (Kashiwa, Japan) between January 2007 and December 2010, were retrospectively evaluated (Fig. 1). Demographics, clinical symptoms

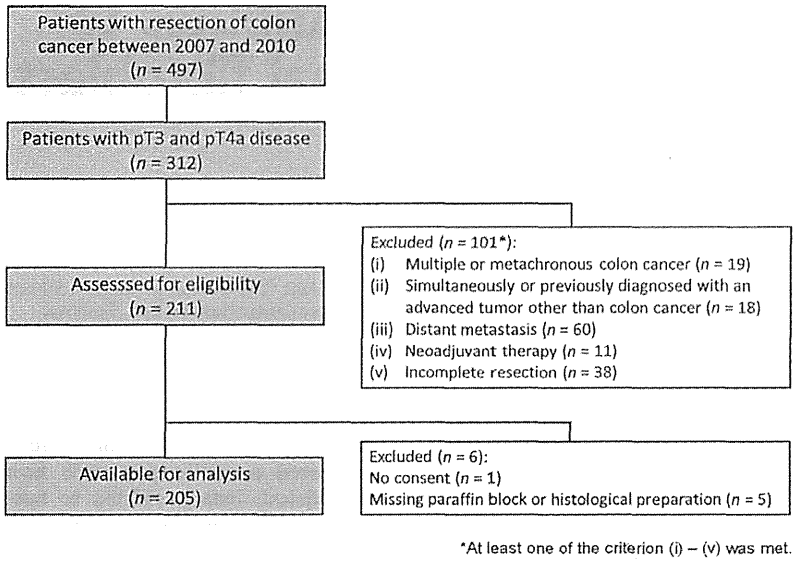

Fig. 1. Flow diagram of the study of colon cancer patients with pT3 and pT4a disease who underwent curative surgery between January 2007 and December 2010. *At least one of the criteria (i–v) was met.

and treatments, serum data, colonoscopy findings, and histopathology and prognostic outcome data for the patients were recorded. Clinical symptoms included abdominal pain, abdominal distension, and vomiting. Treatment of bowel obstruction, including fasting and infusion or decompression with an ileus tube, was carried out according to the severity of the patient's condition. No passage of colonoscope was defined as the inability of an experienced endoscopist to pass a thin scope (φ11.5 mm) beyond a tumor site to the oral-sided colon, and was recorded as one of the features of bowel obstruction.

All cases were reclassified based on the 7th edition of the Union for International Cancer Control TNM staging system.[10] We did not categorize isolated tumor deposits as lymph node metastases to evaluate independently. Follow-up after surgery was carried out in all patients and was comprised

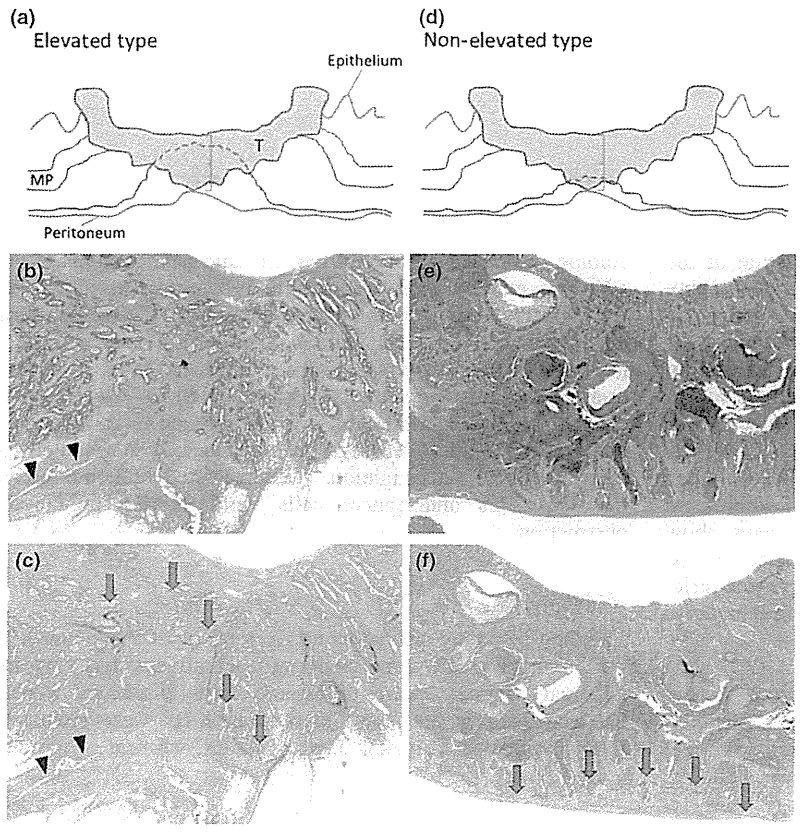

Fig. 2. Two types of elastic lamina invasion (ELI)-positive cases of colon cancer. ELI-positive cases were divided into elevated type (a) and non-elevated type (d) based on whether or not the peritoneal elastic lamina (PEL) was elevated to the surface by more than half the distance of the tumor invasion. H&E staining (b, ×20) and elastica staining (c, ×20) of the elevated type. H&E staining (e, ×20) and elastica staining (f, ×20) of the non-elevated type. Red line represents PEL (a, d). Arrow heads indicate cleft (b, c). Arrows indicate PEL (c, f). MP, muscularis propria; T, tumor.

of serum tumor marker measurement every 3 months and chest and abdominal computed tomography (CT) every 6 months for the first 3 years, then every 6 months for the next 2 years. All patients were followed up from the date of surgery to the last contact (death or last follow-up). Metastasis and local recurrence were considered as tumor recurrence, and the final diagnosis was made by imaging (CT, magnetic resonance imaging, and/or PET-CT), cytology, or biopsy.

Written informed consent for tissue collection and use for research was obtained. The conduct of the study was approved by our local ethics committee (National Cancer Center Hospital; no. 2013-293).

Histopathological analysis. We used the same histopathological examination protocol as that used in our previous study.[6] The resected specimens were fixed in 10% formalin, and the entire tumor was cut into 5-mm slices. Representative slices were embedded in paraffin, cut into 3-μm sections and stained with H&E and elastica stain to evaluate ELI status and lymphovascular invasion. Because of discrimination of the peritoneal elastic lamina (PEL) from the retroperitoneal fascia, we confirmed the continuity from the PEL found at the other area of colonic wall. Therefore, we undertook elastica stain on at least one whole slice where the tumor was closest to the peritoneal surface. The median numbers of H&E and elastica stained sections were 8.0 (range, 2–27) and 5.0 (range, 2–16), respectively.

Cases with tumor invasion beyond the PEL were defined as ELI-positive. First, we divided patients into ELI-positive and ELI-negative cases to identify the difference of clinical features based on the ELI status. Additionally, ELI-positive cases were divided into elevated type or non-elevated type. Cases with the PEL elevation to the surface of more than half the distance of the tumor invasion were regarded as ELI-positive elevated type (Fig. 2). Then, the association between the clinicopathological findings and the three tumor types (ELI-negative, ELI-positive non-elevated type, and ELI-positive elevated type) were assessed.

Azan staining, immunohistochemistry, and computer-assisted image analysis. Two consecutive sections of 4-μm thick slices were obtained from paraffin-embedded blocks, which included all layers of the intestinal wall and tumor area with the deepest infiltration. One section was used for immunohistochemical α-smooth muscle actin (α-SMA) staining (×200, clone 1A4; Dako, Carpinteria, CA, USA) and the other for Azan staining. Immunostaining was carried out using an autostainer (Ventana Benchmark; Roche Diagnostics, Tokyo, Japan), as described previously.[9] High-resolution slide images from each H&E, α-SMA, and Azan stained section were obtained using a Nano Zoomer 2.0-HT slide scanner (Hamamatsu Photonics, Hamamatsu, Japan). All sections were examined using viewer software (NDP View; Hamamatsu Photonics). We divided the tumor area into two equal parts of shallow and deep areas. Five fields with the highest α-SMA and Azan expressions were randomly selected from the shallow and deep layer of each tumor (a total of 10 fields per specimen). Then, images of ×40 magnification (0.59 mm^2) were saved as JPEG files. The ratios of the α-SMA and Azan positive area in the images were calculated using morphometric software (WinRoof; Mitani, Fukui, Japan), as described previously.[9]

Cell cultures and cell lines. Both SPFs and submucosal fibroblasts (SMFs) were obtained from normal sigmoid colon tissue of three patients operated on for sigmoid CC as described previously.[9] The samples were routinely maintained in MF-medium (Toyobo, Tokyo, Japan) at 37°C in a humid atmosphere containing 5% CO_2.

The human colonic cancer cell line DLD-1 was obtained from ATCC (Manassas, VA, USA), and maintained in DMEM (Sigma-Aldrich, St. Louis, MO, USA) containing 100 U/mL penicillin and 100 μg/mL streptomycin (Sigma-Aldrich) and 10% FBS (Gibco, Palo Alto, CA, USA).

Preparation of cancer cell-conditioned medium. Cancer cell-conditioned medium (CCCM) from DLD-1 was obtained as described previously.[9] Initially, $1.7 \times 10^4/cm^2$ of DLD-1 was grown in maintained medium for 48 h, and then starved in DMEM for 24 h. The medium was removed and used as CCCM.

Collagen gel contraction assay. A standard kit assay was used to investigate the difference of contractile ability in fibroblasts (Cell Biolabs, San Diego, CA, USA).[11] Briefly, $1.0 \times 10^5/mm^3$ fibroblasts were mixed with a cold collagen gel solution, then 0.5 mL fibroblast–collagen mixture was added per well in a 24-well plate, and incubated for 1 h at

Table 1. Clinical characteristics according to elastic laminal invasion (ELI) status in patients who underwent primary resection for pT3 and pT4a colon cancer (n = 205)

	ELI(−) n = 113	ELI(+) n = 92	P-value
Age, years			
Median (range)	68 (24–90)	64 (38-89)	0.051
Sex			
Male	51	46	0.488
Female	62	46	
Body mass index, kg/m^2			
Median (range)	23.3 (16.2–34.2)	22.5 (14.5–39.3)	0.141
Total protein level, g/dL			
Median (range)	6.8 (5.4–7.9)	6.8 (5.2–7.9)	0.886
Albumin level, g/dL			
Median (range)	4.1 (2.4–4.8)	4.0 (2.7–5.0)	0.821
C-reactive protein level, mg/dL			
Median (range)	0.10 (0.01–6.46)	0.12 (0.01–5.10)	0.867
White blood cell count, $/mm^3$			
Median (range)	5700 (3200–11 800)	5850 (3200–12 000)	0.571
Neutrophil count, $/mm^3$			
Median (range)	3429 (1728–8626)	3485 (1141–9821)	0.551
Lymphocyte count, $/mm^3$			
Median (range)	1693 (776–3493)	1736 (773–5064)	0.758
Hemoglobin concentration, g/dL			
Median (range)	12.7 (6.9–17.7)	12.7 (7.6–16.7)	0.712
CEA level, ng/mL			
Median (range)	3.6 (0.6–358.9)	3.4 (0.7–197.0)	0.401
Tumor location			
Right	40	22	0.193
Transverse	17	18	
Left	56	52	
Abdominal symptoms			
+	25	34	0.020
−	88	58	
Passage of colon colonoscope†			
+	91	50	<0.001
−	19	41	
Treatment of bowel obstruction			
+	2	11	0.003
−	111	81	

CEA, carcinoembryonic antigen. †Four patients were missing data.

37°C. After the gel polymerization, 1 mL DMEM containing 100 U/mL penicillin, 100 μg/mL streptomycin, and 10% FBS was added and incubated for 24 h. Next, the medium was removed from the plate, and CCCM was added to three wells of each fibroblast type. As a control, serum-free DMEM was added to another three wells. Twenty-four hours later, each gel was gently released from the sides of wells, and pictures were taken another 48 h later. The area of the gel was measured using morphometric software (WinRoof; Mitani), and the contraction rate was obtained by the division of the gel area with CCCM stimulation by the initial gel area.

Statistical analysis. Differences in the clinicopathological features between ELI-positive and ELI-negative cases were assessed using Fisher's exact test and the Mann–Whitney *U*-test; α-SMA and Azan positive area ratios were compared using Student's *t*-test.

Recurrence-free survival (RFS) was defined as the time that elapsed between the date of surgery and any relapse or the last contact. Kaplan–Meier survival curves were plotted and compared using the log–rank test.

All statistical analyses were carried out using SPSS 22 (SPSS, Chicago, IL, USA). All *P*-values were reported as two sided, and statistical significance was defined as $P < 0.05$.

Results

Association between clinical characteristics and ELI status. In the dataset, 92 patients (44.9%) were identified as ELI-positive. Serum data, nutritional status, level of tumor marker, and tumor location were not associated with ELI status (Table 1). However, patients with ELI-positive tumors more frequently complained of clinical symptoms and required treatment for bowel obstruction. No passage of the colonoscope was also found more frequently in ELI-positive cases. For a detailed analysis, dividing ELI-positive cases into two types, clinical findings related to bowel obstruction were found more frequently in the ELI-positive elevated type than in the ELI-positive non-elevated type cases (Fig. 3). Furthermore, patients with ELI-positive elevated type tumors required more treatment for bowel obstruction compared to patients with ELI-negative or ELI-positive non-elevated type tumors.

Association between histopathological characteristics and ELI status. Thirty-eight percent of patients with pT3 disease ($n = 70$) and all patients with pT4a disease ($n = 22$) were ELI-positive. Histopathological findings by tumor type are shown in Table 2. Thin ulcers and thickening under the muscular layer were identified as morphological changes associated with an ELI-positive state. The ELI-positive type was also significantly associated with an invasive infiltrating pattern, a higher pathological nodal stage, a high budding grade, a high lymphovascular invasion grade, and a high perineural invasion grade; features that are related to tumor malignancy. Furthermore, tumor size and annularity rate significantly increased in the ELI-positive elevated type cases. These clinicopathological results suggested that elevation of PEL was associated with bowel obstruction and occurred in parallel with tumor progression.

Association between fibrosis and ELI status. Fibrosis in CRC is associated with bowel obstruction.[12–14] Therefore, we quantitatively assessed fibrosis in tumor tissue using morphometry on Azan and α-SMA staining, which was evaluated by tumor type.

The α-SMA expression was higher in order of ELI-positive elevated type, ELI-positive non-elevated type, and ELI-negative

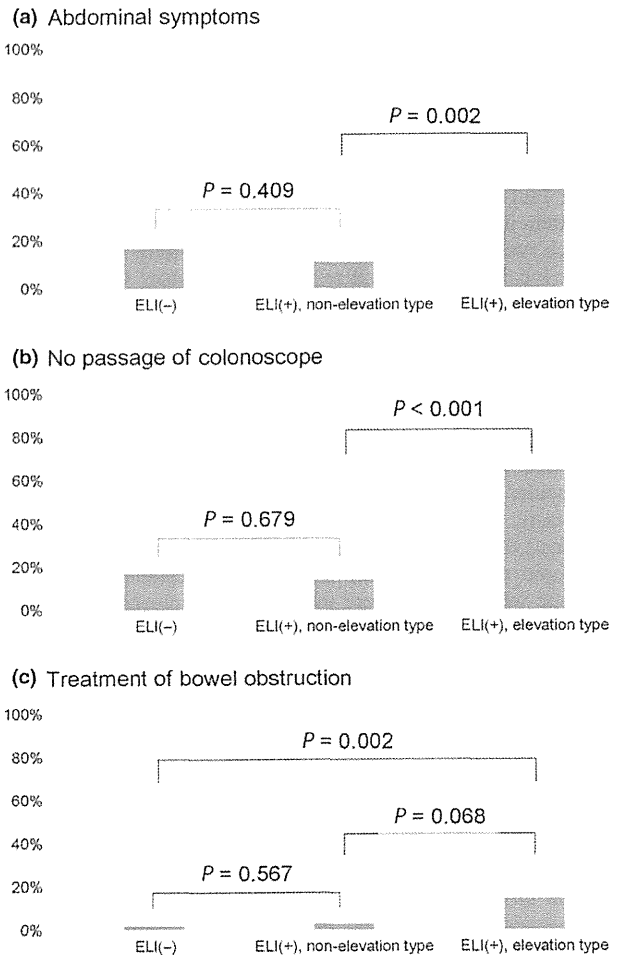

Fig. 3. Incidence rates of clinical findings by colon cancer tumor type. Clinical findings included abdominal symptoms (a), no passage of the colonoscope (b), and treatment of bowel obstruction (c). Tumor types were divided into elastic lamina invasion (ELI)-negative type, elevated type ELI-positive cases, and non-elevated type ELI-positive cases.

cases (Fig. 4a,b). An increase of α-SMA positive area ratio was strongly associated with ELI status, and it was observed not only in the deep tumor area but also in the shallow tumor area. Furthermore, there was a significant difference in the ratio between ELI-positive elevated type and ELI-positive non-elevated type, especially in the shallow tumor area. In the Azan stain, the fibrosis area was also higher in ELI-positive cases than in ELI-negative cases, but the ratio was not different between ELI-positive elevated type and ELI-positive non-elevated type (Fig. 4a,c).

Association between prognosis and ELI status. The median follow-up was 4.3 years (range, 0.3–6.6 years). The 3-year RFS rates for ELI-negative and ELI-positive patients were 95.4% and 74.9%, respectively, and the log–rank analysis revealed a statistically significant difference ($P < 0.001$; Fig. 5a). However, the 3-year RFS rates for ELI-positive non-elevated type and ELI-positive elevated type were 72.2% and 76.7%, respectively, and there was no significant difference between these two types among ELI-positive patients ($P = 0.340$; Fig. 5b).

Contractile ability of SPFs. To estimate the contribution of SPFs to bowel obstruction, contraction assays were carried out and contractile abilities were compared with those of SMFs.

Table 2. Clinical and histopathological findings by tumor type in patients who underwent primary resection for pT3 and pT4a colon cancer (n = 205)

	1. ELI(−) n = 113	2. ELI(+) Non-elevated type n = 36	3. ELI(+) Elevated type n = 56	P-value (1. *vs* 2.)	P-value (2. *vs* 3.)
Maximum transverse tumor size, cm					
Median (range)	4.0 (1.0–10.0)	3.4 (1.0–9.2)	5.0 (2.0–10.5)	0.250	0.003
Maximum longitudinal tumor size, cm					
Median (range)	3.5 (1.0–10.0)	3.0 (1.5–8.0)	4.0 (2.0–8.0)	0.153	0.021
Tumor annularity rate, %					
Median (range)	63.3 (17.6–100)	53.3 (18.8–100)	100 (28.6–100)	0.512	<0.001
Thickness of ulcer, mm					
Median (range)	12.0 (4.0–41.0)	8.0 (4.0–40.0)	9.56 (3.0–26.0)	0.001	0.352
Thickness under the muscular layer, mm					
Median (range)	2.5 (0.1–19.0)	3.0 (0.75–46.0)	4.4 (0.25–20.0)	0.058	0.331
Histologic differentiation					
Well/moderately	108	33	54	0.298	0.298
Poorly/mucinous	5	3	2		
Infiltrating pattern					
Expanding	55	4	4	<0.001	0.382
Invasive	58	32	52		
Tumor depth					
pT3	113	26	44	<0.001	0.486
pT4a	0	10	12		
Nodal status					
pN0	66	16	24	0.002	0.668
pN1	43	12	23		
pN2	4	8	9		
Budding grade					
Grade 1	87	20	35	0.041	0.187
Grade 2	18	12	10		
Grade 3	8	4	11		
Tumor deposits					
+	11	6	6	0.197	0.301
−	102	30	50		
Lymphatic invasion					
+	50	24	37	0.019	0.953
−	63	12	19		
Vascular invasion					
+	64	27	37	0.049	0.364
−	49	9	19		
Perineural invasion					
+	24	15	20	0.015	0.566
−	89	21	36		

ELI, elastic laminal invasion.

The response to CCCM stimulation was significantly higher in SPFs than in SMFs (Fig. 6).

Discussion

In this study, we investigated two types of ELI-positive tumors and first detected the progression-dependent elevation of PEL that was associated with bowel obstruction. Elevation of PEL implied a spread of CMPI toward the luminal surface, and further investigation suggested that the activation of SPFs, which normally reside in the subperitoneal outer area of the colonic wall, contributes to obstruction of the bowel. We have reported that CMPI contributes to tumor progression and metastasis through the interaction of SPFs and cancer cells. Tumors were known to form heterogeneous microenvironments and some of these, including CMPI, promote tumor progression and metastasis.[15–18] However, a progression-dependent alteration of such a tumor microenvironment has not been investigated. In this study, we revealed that a progression-dependent spread of the tumor microenvironment to the shallow layer of the tumor tissue resulted in reduced bowel patency. Our findings first suggest that the tumor-promoting microenvironment can contribute not only to tumor progression or metastasis, but also to the deterioration of clinical findings.

The cancer microenvironment consists of a heterogeneous type of stromal cells, and fibroblasts are one of the major sources.[19] Subperitoneal fibroblasts were reported to be sensitive to CCCM stimulation, and the upregulation of contraction-associated genes, including α-*SMA*, by CCCM was one of the specific features of SPFs.[9] An increase in α-SMA expres-

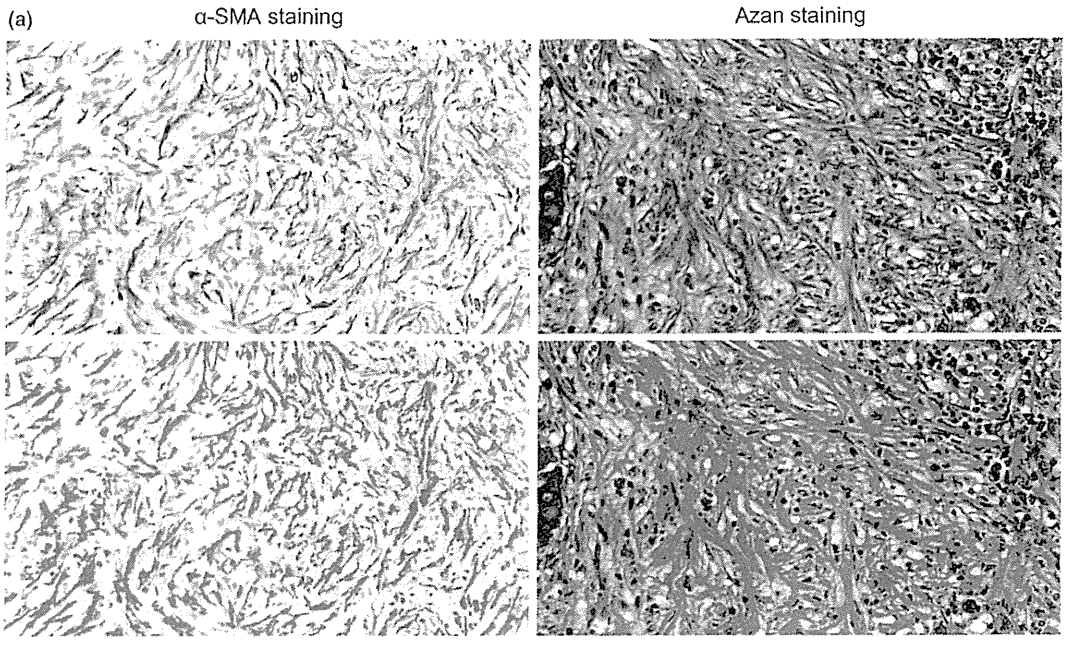

(b) α-SMA staining positive area ratio

Layer	ELI(−)	ELI (+)	
		Non-elevated type	Elevated type
Shallow	11.91% (5.98)	17.68% (5.05)	20.87% (7.05)
Deep	17.68% (6.27)	26.55% (8.89)	28.90% (7.32)
All	14.79% (5.11)	22.11% (5.51)	24.88% (6.02)

(c) Azan staining positive area ratio

Layer	ELI(−)	ELI (+)	
		Non-elevated type	Elevated type
Shallow	32.91% (12.87)	43.83% (14.85)	44.19% (14.20)
Deep	42.24% (11.49)	51.37% (11.64)	50.82% (11.26)
All	37.58% (9.81)	47.60% (11.31)	47.51% (10.88)

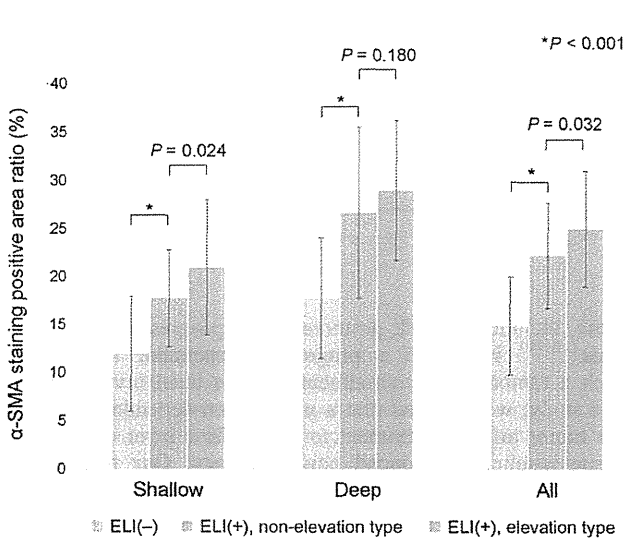

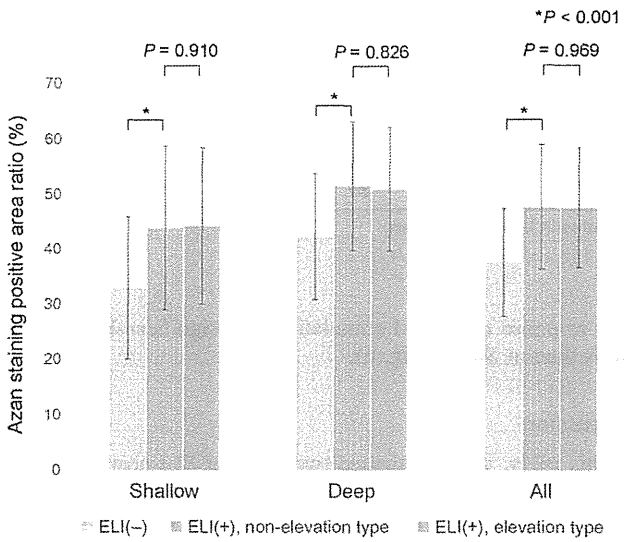

Fig. 4. Association between fibrosis and colon cancer tumor type. α-Smooth muscle actin (α-SMA) staining (×40) and Azan staining (×40) positive areas were successfully detected using morphometric software (a). The α-SMA staining positive area ratio is shown by tumor area (shallow layer, deep layer, and both layers [All]) (b). The Azan staining positive area ratio is also shown (c). Values are mean percentages and those in parentheses are standard deviation. *$P < 0.001$.

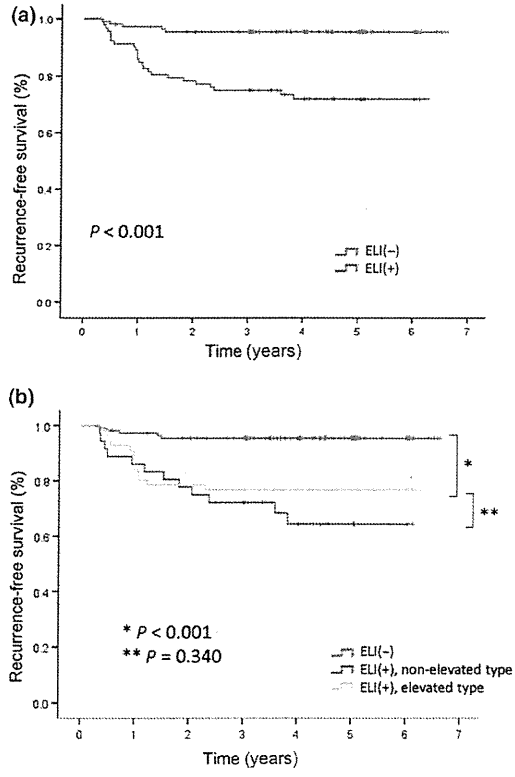

Fig. 5. Kaplan–Meier curves depicting recurrence-free survival of 205 patients who underwent primary resection for pT3 and pT4a colon cancer. (a) Patients were stratified according to elastic laminal invasion (ELI) status. Blue line, ELI-negative cases; red line, ELI-positive cases. (b) Patients were divided into three tumor types. Blue line, ELI-negative type; green, non-elevated type ELI-positive cases; yellow line, elevated type ELI-positive cases.

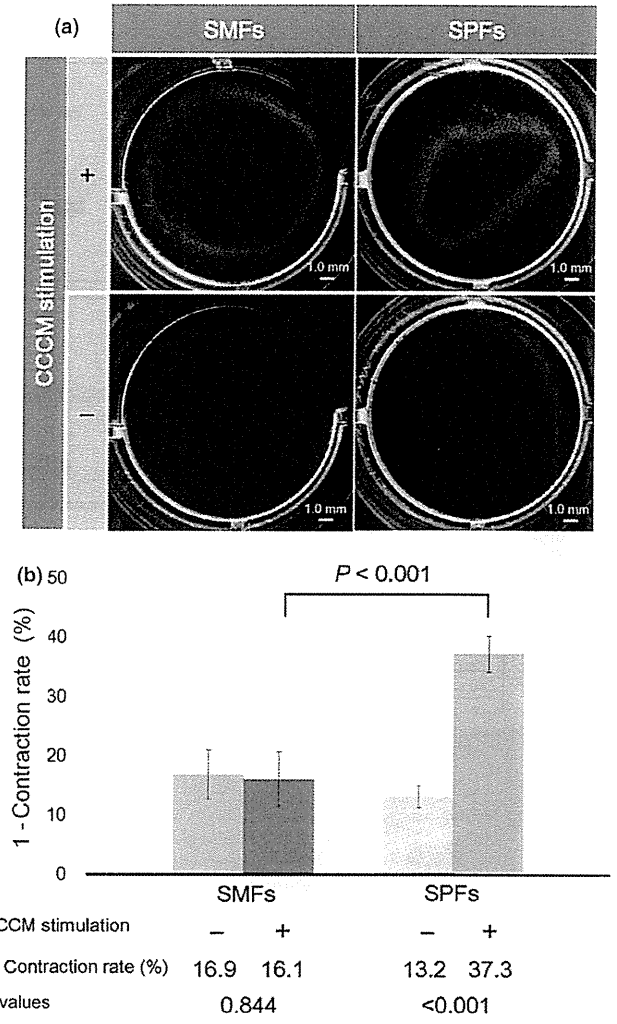

Fig. 6. Contraction assays using submucosal fibroblasts (SMFs) and subperitoneal fibroblasts (SPFs). Gels containing SMFs or SPFs were compared by the presence or absence of cancer cell-conditioned medium (CCCM). (a) Pictures of each gel were taken 48 h after release of each gel from the sides of wells. (b) Contraction rate is shown by bar graph indicating the average value of three gels.

sion was found in CC tissue with strictures and enhanced contractile ability of fibroblasts.[20–22] Concordant with these previous studies, we also found a robust functional contractile ability of SPFs that seemed to be associated with the bowel obstruction. In addition, the spread of CMPI may contribute to the development of clinical findings related to bowel obstruction. However, the spread of this microenvironment did not deteriorate the patient's prognosis. Consequently, the tumor biology would have been already altered by the formation of CMPI, and the spread of CMPI would lead to alteration of tumor morphology.

Morphological alteration in the course of tumor progression has been studied in the early stage of carcinogenesis, as in adenoma–carcinoma sequences and *de novo* cancer. However, there were few studies on the morphological alteration that accompanied the progression of advanced tumor. Recently, we have reported the morphological alteration associated with ELI-positive type invasion.[6] Further detailed analysis in this study revealed that the elevation of the PEL was strongly associated with lateral tumor spread and the resulting increase in tumor annularity rate, which suggested that the spread of CMPI caused morphological alteration. Based on these findings, we propose a model of the morphological alteration that accompanies progression of advanced CC (Fig. 7).

Understanding stromal events may be helpful in the treatment of CRC. More recent research suggests that tumor stroma might be a good target for therapeutic interventions, in particular chemotherapy.[15] For example, it was reported that treatment of pancreatic cancer with nab-paclitaxel reduced the number of cancer-associated fibroblasts in the cancer stroma and improved the response to chemotherapy.[23] Twenty-five percent of patients with uncomplicated CRC with unresectable distant metastasis who underwent chemotherapy required palliative intervention such as bypass surgery, colonic stent, and palliative resection; approximately 80% of these interventions were due to colonic obstruction.[24] We speculate that treatment for tumor stroma improves bowel patency, thereby avoiding stent placement or palliative surgeries that are required for bowel obstruction. Treatments for tumor stroma may be effective in treating patients with unresectable primary CRC to avoid invasive palliative procedures.

The limitation of our study is that there is a difference in the number of H&E and elastica stained slides examined in each case, because we could not adopt the protocol with a predefined number of blocks and sections due to the priority on clinical diagnosis. This might cause a bias in the classification of tumor types.

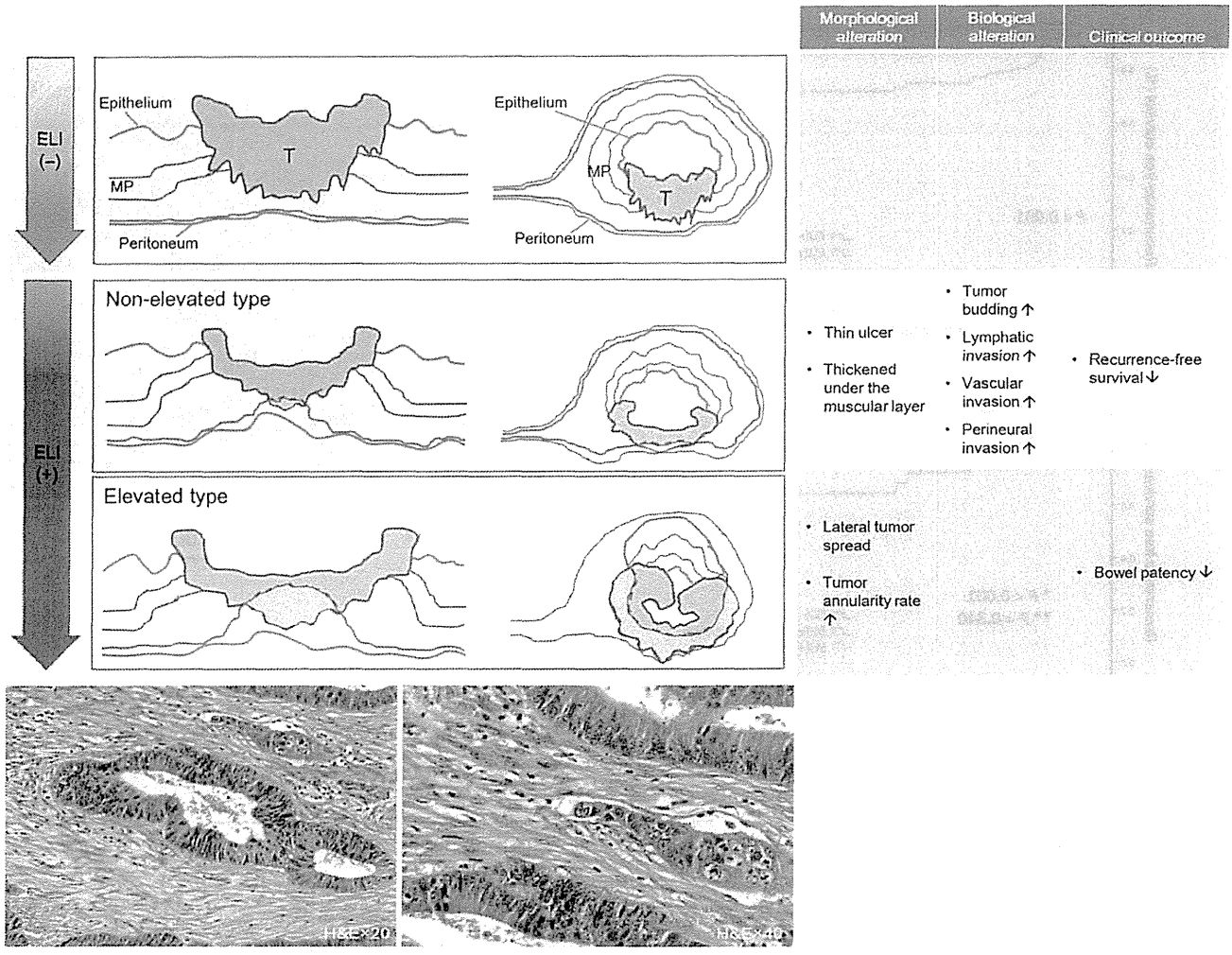

Fig. 7. Proposed model for the tumor progression of colon cancer. Tumor progressed in order of elastic laminal invasion (ELI)-negative type, non-elevated type ELI-positive cases, and elevated type ELI-positive cases. Associations between tumor progression phase and morphological alterations, and biological alterations are described, and the resulting clinical features are shown. The red line represents the peritoneal elastic lamina, and the area filled with yellow represents the cancer microenvironment formed by peritoneal invasion. Histological features of the latter are abundant spindle-shaped fibroblasts and collagen. Higher magnification more clearly revealed spindle-shaped fibroblasts. MP, muscularis propria; T, tumor.

In conclusion, the tumor-promoting microenvironment of CMPI spread into the luminal side of the colonic wall after ELI, and caused bowel obstruction through activation of SPFs. The clinical outcome was affected by CMPI formation, and clinical findings were affected by the spread of CMPI. We are the first group to show that the tumor-promoting microenvironment can spread in the course of tumor progression and can influence physical findings.

Acknowledgment

This study was supported by grants from the Japan Society for the Promotion of Science (Kakenhi 24590458).

Disclosure Statement

The authors have no conflict of interest.

References

1 Ferlay J, Parkin DM, Steliarova-Foucher E. Estimates of cancer incidence and mortality in Europe in 2008. *Eur J Cancer* 2010; **46**: 765–81.
2 Jemal A, Bray F, Center MM, Ferlay J, Ward E, Forman D. Global cancer statistics. *CA Cancer J Clin* 2011; **61**: 69–90.
3 Siegel R, Naishadham D, Jemal A. Cancer statistics, 2012. *CA Cancer J Clin* 2012; **62**: 10–29.
4 Majumdar SR, Fletcher RH, Evans AT. How does colorectal cancer present? Symptoms, duration, and clues to location. *Am J Gastroenterol* 1999; **94**: 3039–45.
5 Hamilton W, Round A, Sharp D, Peters TJ. Clinical features of colorectal cancer before diagnosis: a population-based case–control study. *Br J Cancer* 2005; **93**: 399–405.
6 Kojima M, Nakajima K, Ishii G, Saito N, Ochiai A. Peritoneal elastic laminal invasion of colorectal cancer: the diagnostic utility and clinicopathologic relationship. *Am J Surg Pathol* 2010; **34**: 1351–60.
7 Liang WY, Chang WC, Hsu CY *et al.* Retrospective evaluation of elastic stain in the assessment of serosal invasion of pT3N0 colorectal cancers. *Am J Surg Pathol* 2013; **37**: 1565–70.

8 Yokota M, Kojima M, Nomura S *et al.* Clinical impact of elastic laminal invasion in colon cancer: elastic laminal invasion-positive stage II colon cancer is a high-risk equivalent to stage III. *Dis Colon Rectum* 2014; **57**: 830–8.
9 Kojima M, Higuchi Y, Yokota M *et al.* Human subperitoneal fibroblast and cancer cell interaction creates microenvironment that enhances tumor progression and metastasis. *PLoS One* 2014; **9**: e88018.
10 Sobin LH, Gospodarowicz MK, Wittekind C, eds. *TNM Classification of Malignant Tumors*, 7th edn. West Sussex, UK: Wiley-Blackwell, 2009.
11 Ngo P, Ramalingam P, Phillips JA, Furuta GT. Collagen gel contraction assay. *Methods Mol Biol* 2006; **341**: 103–9.
12 Ueyama T, Yao T, Nakamura K, Enjoji M. Obstructing carcinomas of the colon and rectum: clinicopathologic analysis of 40 cases. *Jpn J Clin Oncol* 1991; **21**: 100–9.
13 Miura S, Kodaira S, Hosoda Y. Immunohistologic analysis of the extracellular matrix components of the fibrous stroma of human colon cancer. *J Surg Oncol* 1993; **53**: 36–42.
14 Miyamoto S, Boku N, Fujii T *et al.* Macroscopic typing with wall stricture sign may reflect tumor behaviors of advanced colorectal cancers. *J Gastroenterol* 2001; **36**: 158–65.
15 Lorusso G, Ruegg C. The tumor microenvironment and its contribution to tumor evolution toward metastasis. *Histochem Cell Biol* 2008; **130**: 1091–103.
16 Alphonso A, Alahari SK. Stromal cells and integrins: conforming to the needs of the tumor microenvironment. *Neoplasia* 2009; **11**: 1264–71.
17 Hanahan D, Weinberg RA. Hallmarks of cancer: the next generation. *Cell* 2011; **144**: 646–74.
18 Quail DF, Joyce JA. Microenvironmental regulation of tumor progression and metastasis. *Nat Med* 2013; **19**: 1423–37.
19 Schmitt-Graff A, Desmouliere A, Gabbiani G. Heterogeneity of myofibroblast phenotypic features: an example of fibroblastic cell plasticity. *Virchows Arch* 1994; **425**: 3–24.
20 Tomasek JJ, Gabbiani G, Hinz B, Chaponnier C, Brown RA. Myofibroblasts and mechano-regulation of connective tissue remodelling. *Nat Rev Mol Cell Biol* 2002; **3**: 349–63.
21 Otranto M, Sarrazy V, Bonte F, Hinz B, Gabbiani G, Desmouliere A. The role of the myofibroblast in tumor stroma remodeling. *Cell Adh Migr* 2012; **6**: 203–19.
22 Hinz B. Matrix mechanics and regulation of the fibroblast phenotype. *Periodontol 2000* 2013; **63**: 14–28.
23 Alvarez R, Musteanu M, Garcia-Garcia E *et al.* Stromal disrupting effects of nab-paclitaxel in pancreatic cancer. *Br J Cancer* 2013; **109**: 926–33.
24 Yun JA, Park Y, Huh JW *et al.* Risk factors for the requirement of surgical or endoscopic interventions during chemotherapy in patients with uncomplicated colorectal cancer and unresectable synchronous metastases. *J Surg Oncol* 2014; **110**: 839–44.

J Gastroenterol (2014) 49:400–407
DOI 10.1007/s00535-013-0822-1

The Japanese Society of Gastroenterology

ORIGINAL ARTICLE—ALIMENTARY TRACT

Histogenesis and prognostic value of myenteric spread in colorectal cancer: a Japanese multi-institutional study

Hideki Ueno · Kazuo Shirouzu · Hideyuki Shimazaki · Hiroshi Kawachi · Yoshinobu Eishi · Yoichi Ajioka · Kiyotaka Okuno · Kazutaka Yamada · Toshihiko Sato · Takaya Kusumi · Ryoji Kushima · Masahiro Ikegami · Motohiro Kojima · Atsushi Ochiai · Akihiko Murata · Yoshito Akagi · Takahiro Nakamura · Kenichi Sugihara · Study Group for Perineural Invasion projected by the Japanese Society for Cancer of the Colon and Rectum (JSCCR)

Received: 14 February 2013 / Accepted: 28 March 2013 / Published online: 16 May 2013

Abstract
Background The histogenesis of the pattern of cancer spread along Auerbach's plexus (myenteric spread: MS) remains unclear and its prognostic value in colorectal cancer (CRC) has not been thoroughly investigated.
Methods Pathology slides of 2845 pT2/pT3/pT4 CRCs stained with hematoxylin–eosin (H&E) were reviewed at 10 institutions. MS was classified into 2 groups depending on whether it was accompanied by the finding of perineural invasion (PN) within the lesion. In addition, immunohistochemical staining (D2-40, S100, CD56, synaptophysin) was performed for serially sectioned specimens from 50 CRCs diagnosed as having PN-negative MS.
Results MS was observed in 504 patients (17.7 %); 360 patients were classified as having PN-positive MS and 144 as having PN-negative MS. The 5-year disease-free survival rate of patients with MS was lower than that of patients without MS (63.3 vs 82.7 %, $P < 0.0001$); however, there was no significant difference in survival outcome according to the presence or absence of intralesion PN in MS. Multivariate analysis showed that the prognostic impact of MS was independent of conventional prognosticators including T and N stages, vascular invasion and extramural PN. In all the tumors having PN-negative MS, remnants of neural tissue were identified within or around cancer nests located at the leading edge of MS.
Conclusions MS is an important prognostic factor for CRC. This feature is the result of cancer development with replacement of Auerbach's plexus and can be classified as intramural PN. The clinical significance of "Pn1" in the UICC/AJCC TNM classification could be enhanced by individual assessment both intramurally and extramurally.

H. Ueno (✉)
Department of Surgery, National Defense Medical College, 3-2 Namiki, Tokorozawa, Saitama 359-8513, Japan
e-mail: ueno@ndmc.ac.jp

K. Shirouzu · Y. Akagi
Department of Surgery, Kurume University Faculty of Medicine, Kurume, Japan

H. Shimazaki
Department of Laboratory Medicine, National Defense Medical College, Tokorozawa, Japan

H. Kawachi · Y. Eishi
Department of Human Pathology, Tokyo Medical and Dental University, Tokyo, Japan

Y. Ajioka
Division of Molecular and Diagnostic Pathology, Graduate School of Medical and Dental Sciences, Course for Molecular and Cellular Medicine, Niigata University, Niigata, Japan

K. Okuno
Department of Surgery, Kinki University School of Medicine, Osakasayama, Japan

K. Yamada
Department of Surgery, Coloproctology Center, Takano Hospital, Kumamoto, Japan

T. Sato
Department of Surgery, Yamagata Prefectural Central Hospital, Yamagata, Japan

T. Kusumi
Department of Surgery, Keiyukai Sappro Hospital, Sapporo, Japan

R. Kushima
Department of Pathology, National Cancer Center Hospital, Tokyo, Japan

Keywords Colorectal cancer · Myenteric spread · Auerbach's plexus · Perineural invasion · The UICC/AJCC TNM classification

Introduction

Perineural invasion (PN) has long been recognized as a clinically important pathological feature of various malignant tumors and is strongly associated with adverse prognostic outcome [1]. In the 7th edition of TNM Classification of Malignant Tumours, the designations of "Pn0" and "Pn1" are applied for tumors with no PN and those with PN, respectively [2]. In the field of colorectal cancer (CRC), the American Joint Committee on Cancer (AJCC) staging manual (seventh edition) recommends PN be recorded as a site-specific prognostic marker in CRC [3]. However, the bowel layer for PN assessment is not clearly referenced, and the assessment of intramural PN in routine pathological practice presumably varies depending on both the institutions and pathologist involved.

Regarding the distribution of intramural PN, it is rarely observed in the submucosal, circular muscle, or longitudinal muscle layers in CRC; however, intramural PN foci are practically observed in the Auerbach's plexus area. Although few studies have investigated the clinical value of PN in Auerbach's plexus, a prospective single-institutional study demonstrated that a distinctive pattern of horizontal cancer spread along the Auerbach's plexus area (myenteric spread) accompanied by PN was associated with adverse prognostic outcome [4]. In addition, myenteric spread was shown to be associated with unfavorable prognostic outcome, irrespective of intralesion PN findings [5].

The actual histogenesis of myenteric spread has not been clarified to date. Although pre-existing structures such as local neural or lymphatic networks may be considered original structures very relevant to this type of cancer development, histological evidence of the tumor utilizing a specific pre-existing structure as a development route has not been consistently detected in lesions. Therefore, whether myenteric spread simply results from a single histogenesis, e.g., PN, or is multifactorial remains unclear.

This multi-institutional study was projected by the Japanese Society for Cancer of the Colon and Rectum (JSCCR) for establishing assessment criteria for determining PN in CRC. In this study, we attempted to clarify the underlying histogenesis of myenteric spread on the basis of prognostic and immunohistochemical analyses and to clarify the clinical implication of this type of cancer spread.

Patients and methods

Patients

In total, 2845 patients with pT2/pT3/pT4 CRC who consecutively underwent curative surgery at 10 JSCCR institutions (Kurume University Faculty of Medicine, National Defense Medical College, Tokyo Medical and Dental University, Takano Hospital, Keiyukai Sapporo Hospital, National Cancer Center Hospital, Jikei University School of Medicine, Hirosaki University School of Medicine, Kinki University School of Medicine, and Yamagata Prefectural Central Hospital) between 1999 and 2004 were analyzed. This dataset included 1695 men and 1150 women (average age 65 years, range 17–96 years). No patient received preoperative chemotherapy or radiotherapy. With regard to adjuvant therapy administered to patients, 1113 patients received chemotherapy, 1658 patients received no adjuvant therapy, and little information on postoperative treatment was available for 74 patients. Chemotherapy with single oral anticancer drugs was the most common postoperative therapy administered (765), followed by 5FU/leucovorin (255) and UFT/leucovorin (56). The average follow-up was 77 months (range 1–149 months) for 2151 survivors.

Histological evaluation of myenteric cancer spread

The pattern of horizontal cancer spread along the Auerbach's plexus zone was defined as myenteric spread (Fig. 1). Myenteric spread was assessed on hematoxylin–eosin (H&E) slides prepared in routine pathological practice and was classified into 2 types depending on whether the lesion was accompanied by the histological finding of PN. PN was defined as the histological finding of tumor cells invading or spreading along nerve fascicles. The status of myenteric spread as well as PN

M. Ikegami
Department of Pathology, Jikei University School of Medicine, Tokyo, Japan

M. Kojima · A. Ochiai
Pathology Division, Research Center for Innovative Oncology National Cancer Center Hospital East, Kashiwa, Japan

A. Murata
Department of Surgery, Hirosaki University School of Medicine, Hirosaki, Japan

T. Nakamura
Laboratory for Mathematics, National Defense Medical College, Tokorozawa, Japan

K. Sugihara
Department of Surgery, Tokyo Medical and Dental University, Tokyo, Japan

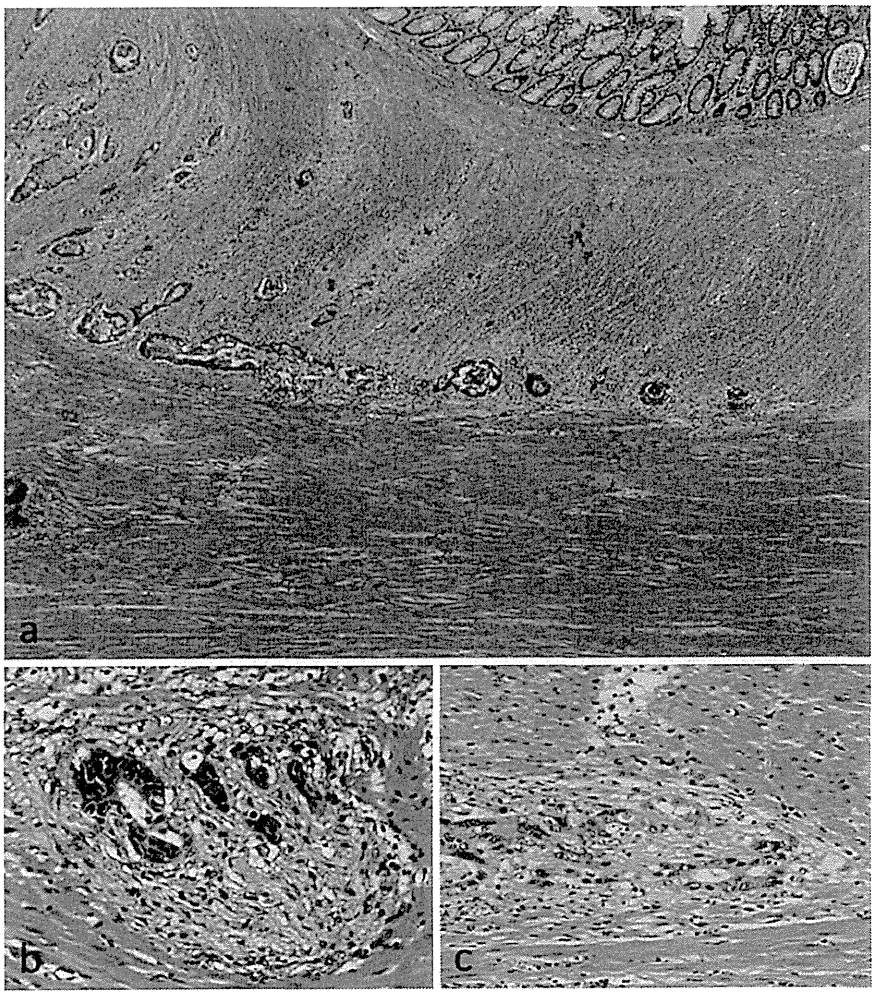

Fig. 1 Myenteric spread in colorectal cancer. **a** Horizontal spread of cancer along the Auerbach's plexus zone was defined as myenteric cancer spread. **b** In a myenteric spread lesion, we observed nerve fascicles associated with cancer cells in certain instances; however, **c** histological findings of neural involvement were not obvious in others. All images, H&E staining (**a** ×4 objective lens; **b**, **c** ×40 objective lens)

external to the muscularis propria (extramural PN) was evaluated at each institution. The consensus for the concept of judging myenteric spread and its classification was kept among institutions participated in this study on the basis of some histological pictures as shown in Fig. 1.

Immunohistochemical staining with neural and lymphatic markers

Serially sectioned slides were prepared from tumors, which had been diagnosed as showing myenteric spread but were unaccompanied by evidence of PN, at 6 institutions (National Defense Medical College, Tokyo Medical and Dental University, Niigata University, Kinki University School of Medicine, Keiyukai Sapporo Hospital, and Yamagata Prefectural Central Hospital). In total, 50 tumors in which myenteric spread was observed (on glass slides newly prepared for immunohistochemical examination) were submitted to the study to clarify the histogenesis of myenteric spread. Immunohistochemical staining was performed on serially sectioned specimens using neural markers (synaptophysin, S100, and CD56) and D2-40 antibody. For tumors in which no positive findings were observed within myenterically spread lesions according to these markers of immunohistochemical staining, serial sectioning and staining were repeatedly performed in the same manner.

Statistical analyses

Correlation between the 2 types of myenteric spread as well as the distribution of myenteric spread and extramural PN was evaluated by the Chi-square test and the *t* test. The disease-free and overall survival rates were calculated on the basis of the Kaplan–Meier method, and differences assessed by the log-rank test. Cox proportional hazards regression analysis was used to determine the impact of prognostic parameters on disease-free survival. Statistical calculations were performed using StatView ver. 5.0 software (SAS Institute, Cary, NC, USA) and SPSS software package (SPSS, Inc., Chicago, IL, USA).

Results

Incidence and prognostic impact of myenteric spread

Myenteric spread was observed in 504 patients (17.7 %). It was significantly associated with T and N stages as well as with conventional histological parameters such as tumor differentiation, lymphatic invasion, venous invasion, and extramural PN (Table 1).

The incidence of myenteric spread differed according to the location of the primary tumor (Fig. 2). The incidence of myenteric spread was lower in the cecum and lower rectum than in other parts of the large bowel. In contrast, the incidence of extramural PN was higher in the rectum than in the colon.

Myenteric spread exerted a significant adverse effect on postoperative disease-free survival and overall survival (Fig. 3). Multivariate Cox proportional analysis showed that the prognostic impact of myenteric spread was independent of conventional prognostic markers including tumor differentiation, T stage, N stage, vascular invasion and extramural PN (Table 2).

Comparison of myenteric spread in relation to evidence of intralesion PN

Among tumors showing myenteric spread, 360 tumors had evidence of PN in the myenteric spread lesion on H&E slides, whereas such finding could not be observed in 144 tumors. Conventional parameters associated with metastatic potential such as N status, tumor grade, vascular invasion, and extramural PN did not differ according to the presence of PN in lesions with myenteric spread, although myenteric spread with positive evidence of PN was less frequently detected in larger tumors and in those invading the deeper layers (Table 1). Tumor

Table 1 Clinicopathological background of tumors showing myenteric spread

	Overall ($N = 2845$)			Tumors with myenteric spread ($N = 504$)		
	Myenteric spread			Finding of PN on H&E slides		
	Absence (2341)	Presence (504)	P value	Absence (144)	Presence (360)	P value
Gender						
Male	1390 (82.0)	305 (18.0)	0.6363	86 (28.2)	219 (71.8)	0.8177
Female	951 (82.7)	199 (17.3)		58 (29.1)	141 (70.9)	
Tumor location						
Right colon	671 (84.7)	121 (12.3)	0.0001	40 (33.1)	81 (66.9)	0.2551
Left colon	949 (78.8)	256 (21.2)		74 (28.9)	182 (71.1)	
Rectum	721 (85.0)	127 (15.0)		30 (23.6)	97 (76.4)	
Tumor diameter	49.2	48.8	0.7870	51.7	47.7	0.0475
T stage						
T2	525 (95.3)	26 (4.7)	<0.0001	4 (15.4)	22 (84.6)	0.0040
T3	1370 (81.1)	320 (18.9)		80 (25.0)	240 (75.0)	
T4	446 (73.8)	158 (26.2)		60 (38.0)	98 (62.0)	
N stage						
N0	1478 (88.5)	192 (11.5)	<0.0001	65 (33.9)	127 (66.1)	0.1166
N1	664 (76.4)	205 (23.6)		51 (24.9)	154 (75.1)	
N2	199 (65.0)	107 (35.0)		28 (26.2)	79 (73.8)	
No. of LN examined	24.6	24.6	0.9384	24.9	24.5	0.8182
Tumor differentiation						
G1	1143 (84.9)	203 (15.1)	0.0010	61 (30.0)	142 (70.0)	0.1592
G2	1047 (79.4)	271 (20.6)		79 (29.2)	192 (70.8)	
G3	151 (83.4)	30 (16.6)		4 (13.3)	26 (86.7)	
Lymphatic invasion						
Negative	836 (90.0)	93 (10.0)	<0.0001	26 (28.0)	67 (72.0)	0.8845
Positive	1505 (78.5)	411 (21.5)		118 (28.7)	293 (71.3)	
Venous invasion						
Negative	987 (84.9)	176 (15.1)	0.0027	49 (27.8)	127 (72.2)	0.7903
Positive	1354 (80.5)	328 (19.5)		95 (29.0)	233 (71.0)	
Extramural PN						
Negative	2177 (86.0)	353 (14.0)	<0.0001	99 (28.2)	254 (72.0)	0.6893
Positive	164 (52.1)	151 (47.9)		45 (29.4)	106 (70.2)	

PN perineural invasion, *H&E* hematoxylin and eosin, *LN* lymph node